Colloids and Surfaces B: Biointerfaces 159 (2017) 586–595

Contents lists available at ScienceDirect

Colloids and Surfaces B: Biointerfaces

journal homepage: www.elsevier.com/locate/colsurfb

Full Length Article

Dual delivery nanosystem for biomolecules. Formulation, characterization, and *in vitro* release

Inmaculada Ortega-Oller[a,1], Teresa del Castillo-Santaella[b,1], Miguel Padial-Molina[a], Pablo Galindo-Moreno[a], Ana Belén Jódar-Reyes[b], José Manuel Peula-García[b,c,*]

[a] Department of Oral Surgery and Implant Dentistry, University of Granada, Granada, Spain
[b] Biocolloid and Fluid Physics Group, Department of Applied Physics, University of Granada, 18071 Granada, Spain
[c] Department of Applied Physics II, University of Malaga, 29071 Malaga, Spain

ARTICLE INFO

Article history:
Received 25 May 2017
Received in revised form 18 July 2017
Accepted 17 August 2017

Keywords:
PLGA
Nanoparticles
Protein encapsulation
Release

ABSTRACT

Because of the biocompatible and biodegradable properties of poly (lactic-co-glycolic acid) (PLGA), nanoparticles (NPs) based on this polymer have been widely studied for drug/biomolecule delivery and long-term sustained-release. In this work, two different formulation methods for lysozyme-loaded PLGA NPs have been developed and optimized based on the double-emulsion (water/oil/water, W/O/W) solvent evaporation technique. They differ mainly in the phase in which the surfactant (Pluronic® F68) is added: water (W-F68) and oil (O-F68). The colloidal properties of these systems (morphology by SEM and STEM, hydrodynamic size by DLS and NTA, electrophoretic mobility, temporal stability in different media, protein encapsulation, release, and bioactivity) have been analyzed. The interaction surfactant-protein depending on the formulation procedure has been characterized by surface tension and dilatational rheology. Finally, cellular uptake by human mesenchymal stromal cells and cytotoxicity for both systems have been analyzed.

Spherical hard NPs are made by the two methods However, in one case, they are monodisperse with diameters of around 120 nm (O-F68), and in the other case, a polydisperse system of NPs with diameters between 100 and 500 nm is found (W-F68). Protein encapsulation efficiency, release and bioactivity are maintained better by the W-F68 formulation method. This multimodal system is found to be a promising "dual delivery" system for encapsulating hydrophilic proteins with strong biological activity at the cell-surface and cytoplasmic levels.

1. Introduction

Tissue regeneration is a complex biological action involving multiple steps in a sequential, ordered, and controlled manner [1,2]. Classically, bioactive molecules have been proposed to aid in these processes. However, the use of high doses, denaturation and loss of biological activity, uncontrolled timing of action, and diffusion to other tissues have been highlighted as major issues of this therapeutic strategy [3]. To help solve these problems, nanomedicine has been intensively investigated in recent years as an emerging area. This involves diagnostic, therapeutic, and regeneration methods by means of structures and systems in which size and shape are controlled at the atomic, molecular, and supramolecular levels [4]. The transport and controlled delivery of drugs and/or therapeutic biomolecules improve their pharmacokinetics and pharmacodynamics and, at the same time, minimize harmful side effects. For these purposes, different nanosystems have been described. Poly lactic-co-glycolic acid (PLGA) exhibits low cytotoxicity as well as high biocompatibility and biodegradability with the release of non-toxic by-products [5].

In the last decade, the use of PLGA has been investigated to deliver a wide spectrum of active agents, from hydrophobic drug molecules [6–8] to hydrophilic biomolecules as peptides [9], proteins [10–15] or nucleic acids [16,17]. These delivery systems have been produced via different formulation processes for their application in both systemic and local site-specific therapies [18].

* Corresponding author at: Department of Applied Physics II, University of Málaga, 29071 Málaga, Spain.
E-mail address: jmpeula@uma.es (J.M. Peula-García).
[1] Both authors contributed equally to this work.

http://dx.doi.org/10.1016/j.colsurfb.2017.08.027
0927-7765/

However, their design and development as nanocarriers are difficult due to the problematic release pattern when the encapsulated molecules are proteins for which initial bursts and slow or incomplete release might be a problem [18–20]. Moreover, the specific conditions of the release may need to be different depending on the final application of the nanocarrier [20,21].

The water-in-oil-in-water (W/O/W) double emulsion technique is the most widely used protein-encapsulation method for PLGA micro- (MP) and nanoparticles (NP) [22,23]. It allows different factors to be modulated such as the type of PLGA, the use of other polymers blended with PLGA, the addition of surfactants, the mechanical stress or the organic solvent [20]. It is also possible to construct several types of co-polymers to modify the hydrophobicity:hydrophilicity ratio [18,24] and the colloidal stability, size, and release process. PLGA/polyethylene glycol pair and surfactants such as polyvinyl alcohol (PVA) or polyethylene oxides (PEO) are the most widely studied [7,12,25,26]

On the other hand, tissue engineering requires the participation of mesenchymal stromal cells (MSCs) [27]. MSCs are known to have the ability to differentiate into multiple cell types, including osteoblasts. Osteoblasts are the main cells responsible for synthesizing the mineralized compartment of bone tissue. This process is regulated by, among other molecules, BMP-2 [3]. PLGA particles loaded with BMP-2 have been extensively used, as has been described and reviewed elsewhere [3,28–31].

Thus, within this context, it was the aim of the current study to optimize the formulation and properties of a nanoparticle system with potential therapeutic applications. Two different strategies to obtain PLGA-surfactant NPs were tested, by using lysozyme as a model for BMP-2. The size and morphology, polydispersity index, zeta potential, colloidal stability, and encapsulation efficiency (EE) of the protein were analyzed.

Once the physico-chemical characterization was completed, the study was focused on the protein-release process, using different techniques to study the results of *in vitro* experiments and focusing it on the release pattern and the biological activity of the lysozyme released. In this way, a new formulation was established to develop a PLGA nanosystem with a singular dual size distribution and the adequate balance between encapsulation and release of biologically active proteins. Finally, the effects of the proposed PLGA system were tested on primary MSCs *in vitro* as a proof of concept.

2. Materials and methods

2.1. Formulation of the nanoparticles

Poly(lactide-co-glycolide) acid (PLGA 50:50) ([C_2 H_2 O_2]x [C_3 H_4 O_2]y) x = 50, y = 50 (Resomer® 503H), 32–44 kDa was used as the polymer. The polymeric surfactant Pluronic® F68 (Poloxamer 188) (Sigma-Aldrich) was used as the emulsifier. The structure is based on a poly(ethylene oxide)-block-poly(propylene oxide)-block-poly(ethylene oxide) and it is expressed as PEOa-PPOb-PEOa with a = 75 and b = 30. Lysozyme from chicken egg white (Sigma-L7651) was used as hydrophilic protein. Water was purified in a Milli-Q Academic Millipore system. Two different formulation methods were developed, termed O-F68 and W-F68.

In the O-F68 method, 25 mg of PLGA and 15 mg of F68 were dissolved in 660 μL of dichloromethane (DMC) and vortexed. Then, 330 μL of acetone were added and vortexed. Next, 100 μL of a buffered solution at pH 12.8, with or without lysozyme (5 mg/mL), were added dropwise while vortexing for 30 s. Immediately, this primary water/oil (W/O) emulsion was poured into a glass containing 12.5 mL of ethanol under magnetic stirring, and 12.5 mL of MilliQ water were added. After 10 min of magnetic stirring, the organic solvents were rapidly extracted by evaporation under vacuum until the sample reached a final volume of 10 mL.

In the W-F68 method, 100 mg of PLGA were dissolved in a tube containing 1 mL of ethyl acetate (EA) and vortexed. 40 μL of a buffered solution at pH 12.8, with or without lysozyme (20 mg/mL), were added and immediately sonicated (Branson Ultrasonics 450 Analog Sonifier), fixing the *Duty cycle* dial at 20% and the *Output control* dial at 4, for 1 min with the tube surrounded by ice. This primary W/O emulsion was poured into a plastic tube containing 2 mL of a buffered solution (pH 12.8) of F68 at 1 mg/mL, and vortexing for 30 s. Then, the tube surrounded by ice was sonicated again at the maximum amplitude for the micro tip (Output control 7), for 1 min. This second W/O/W emulsion was poured into a glass containing 10 mL of the buffered F68 solution and kept under magnetic stirring for 2 min. The organic solvent was then rapidly extracted by evaporation under vacuum to a final volume of 8 mL.

2.2. Cleaning and storage

After the organic solvent evaporation, the sample was centrifuged for 10 min at 20 °C at 14000 or 12000 rpm for O-F68 and W-F68 methods, respectively. The supernatant was filtered using 100 nm filters for measuring the free non-encapsulated protein. The pellet was then resuspended in PB up to a final volume of 4 mL and kept under refrigeration at 4 °C.

2.2.1. Protein loading and encapsulation efficiency

The initial protein loading was optimized for the nanoparticle formulation, preserving the final colloidal stability after the evaporation step and being different for each nanosystem. Also, 1.6% w/w (Lys/PLGA) was used for O-F68 and 0.8% w/w (Lys/PLGA) for W-F68 one. The amount of encapsulated lysozyme was calculated by measuring the difference between the initial amount added and the free non-encapsulated protein, which was tested by bicinchoninic acid assay (BCA, Sigma-Aldrich). Then, protein encapsulation efficiency (EE) and final drug loading (DL) was calculated as follows:

$$EE = \frac{M_I - M_F}{M_I} \times 100 \quad DL = \frac{M_I - M_F}{M_{polymer}} \times 100$$

where M_I the initial total mass of Lys, M_F is the total mass of Lys in the aqueous supernatant, and $M_{polymer}$ is the mass of PLGA in the formulation.

2.3. Characterization of the nanoparticles

2.3.1. Interfacial characterization of the first water-in-oil emulsion

The surface tension and dilatational rheology measurements at the air-water interface were made in the OCTOPUS [32], a Pendant Drop Surface Film Balance equipped with a subphase multi-exchange device (patent submitted P201001588) described in detail elsewhere [33]. Here, air plays the role of the organic phase. The surface tension is calculated with DINATEN® software, based on axisymmetric drop shape analysis (ADSA), and the dilatational modulus (E) of the interfacial layer is determined from image analysis with the program CONTACTO®. The *in vitro* model is described in "Supplementary material".

2.3.2. Particle morphology

Nanoparticles were imaged by Scanning Electron Microscopy (SEM) and Scanning Transmission Electron Microscopy (STEM) using a Zeiss SUPRA 40VP field emission scanning electron microscope from the Centre for Scientific Instrumentation of the University of Granada (CIC, UGR).

2.3.3. Nanoparticle size and electrokinetic mobility

The hydrodynamic diameter and electrophoretic mobility of the NPs were determined by using a Zetasizer NanoZeta ZS device (Malvern Instrument Ltd, U.K.) working at 25 °C with a He-Ne laser of 633 nm and a scattering angle of 173°. Each data point was taken as an average over three independent sample measurements. The size of the NPs was characterized by Dynamic Light Scattering (DLS). The average hydrodynamic diameter (Z-average or cumulant mean), and the polydispersity index (PDI) were computed. These parameters are calculated through a cumulant analysis of the data, which is applicable for narrow monomodal size distributions [34]. We also determined the intensity size distribution from an algorithm provided by the Zetasizer software (General Purpose).

The electrophoretic mobility was determined by the technique of Laser Doppler Electrophoresis. An electrophoretic mobility distribution as well as an average electrophoretic mobility (μ-average) was established for each sample.

The hydrodynamic size distribution of the NPs with wide size distributions from DLS was also measured by using Nanoparticle Tracking Analysis (NTA) in a NanoSight LM10-HS(GB) FT14 (NanoSight, Amesbury, United Kingdom). All samples were measured more than three times for 60 s with manual shutter, gain, brightness, and threshold adjustments at 25 °C. The average size distribution (particle concentration vs. diameter) was calculated as an average of at least three independent size distributions.

2.3.4. Nuclear magnetic resonance (NMR) of the nanoparticles

The 1HNMR spectra of free F68, lysozyme-loaded particles from O-F68 method with and without F68, and lysozyme-loaded particles from W-F68 method were measured with a VNMRS 500 MHz spectrometer (Agilent) in the Centre for Scientific Instrumentation (CIC) of the University of Granada.

2.4. Colloidal and temporal stability in biological media

The average hydrodynamic diameter and the polydispersity index (PDI) by DLS of each system were measured to determine their colloidal stability in different media (Phosphate buffer [PB], Phosphate buffer saline [PBS], and cell culture medium: Dulbecco's modified Eagle's medium, [DMEM] from Sigma) and at different times after (0, 1, and 5 days).

In vitro release experiments were conducted following a similar methodology as described above (*Encapsulation efficiency*) but using 1 mL of each sample suspended in PBS at 37 °C. The protein released from these samples was determined every 24 h by supernatant analysis, and the pellet was suspended in the same volume of buffer to maintain the release conditions. All experiments were developed in triplicate.

2.4.1. Confocal microscopy

Lysozyme was labeled with fluorescein isothiocyanate (FITC) using a method described by Kok et al. [35]. After FITC and lysozyme covalent conjugation, concentrations were estimated spectrophotometrically using the extinction coefficients described for FITC at 494 nm and 280 nm. The lysozyme concentration was calculated measuring optical absorbance at 280 nm and subtracting the corresponding FITC absorbance at this wavelength. Images were made in a Nikon A1 laser scanning confocal microscope from CIC, UGR. All experiments were performed in triplicate and replicated at least twice.

2.5. Biological activity and interactions

2.5.1. Lysozyme biological activity

The biological activity of lysozyme was analyzed by an enzymatic activity kit (Sigma-Aldrich) using *Micrococcus lysodeikticus* cells as the substrate, following the manufacturer's instructions.

2.5.2. Cellular uptake

Primary human mesenchymal stem cells (hMSCs) were taken from healthy maxillary alveolar bone according to previously described protocols [36]. After confirming their phenotype by flow cytometry and trilineage differentiation tests, 12000 cells per well were cultivated in sterile plates with glass bottom (Ibidi cat n° 81158) overnight. These cells were treated with medium without fetal bovine serum (FBS) and Cell Tracker Red (1:5000) (C34552, ThermoFisher) for 30 min. Then, the medium was removed and supplemented with 10% FBS, after which the particles with lysozyme-FITC were added. Then, the hMSCs were incubated 30 min again, washed three times with PBS 1X, and fresh medium supplemented with 2% FBS added. Finally, the hMSCs were examined by a confocal microscope (Nikon Eclipse Ti-E). Cell cultures were in all cases maintained at 37 °C and 5% CO_2 atmosphere.

3. Results and discussion

3.1. Formulation of the nanoparticles

The methods developed in this work are intended to improve the existing formulation techniques for hydrophilic protein loaded-PLGA NPs based on a double-emulsion process [10,22]. The novelty of these methods is the use of the polymeric surfactant F68, either in the organic phase (O-F68 method) or in the aqueous phase (W-F68). This surfactant reduces the size of the NPs, enhances their stability, and protects the encapsulated protein. In addition, the presence of F68 on the surface of the particles reduces the recognition of the nanocarriers by the mononuclear phagocytic system (MPS) [37].

Additionally, the choice of the organic solvent significantly affects the properties of the final colloidal system, since the organic solvent solubility regulates the inner and surface structure of the particle. In addition, the interaction of the solvent with the encapsulated biomolecule can alter its bioactivity as a consequence of its denaturation, as found for methylene chloride [26]. In the O-F68 method, DMC is chosen as the organic solvent due to its lower water solubility to facilitate the emulsification process, and its low boiling point for easy evaporation. However, a freely water-miscible organic solvent (acetone) and the emulsifier F68 were added in this organic phase to reduce its negative biological effects on the encapsulated protein [24]. This emulsifier also reduces the protein-hydrophobic PLGA matrix interaction, and thus the disruption of the protein structure [3]. By contrast, in the W-F68 method, ethyl acetate was used as the organic solvent, which exerts less denaturizing effects on the encapsulated protein [38]. The higher water solubility of this solvent favors rapid solvent removal. The solvent removal rate is also accelerated by increasing the shear stress during the second emulsification step. It also enhances the encapsulation efficiency and minimizes the contact time between the protein and organic solvent [3]. Poloxamer F68 is introduced in the external aqueous phase.

Both formulations (O-F68 and W-F68) (Table 1) gave rise to colloidally stable samples and the encapsulation of lysozyme inside the nanoparticles, in agreement with the double W/O/W emulsion method [23]. Lysozyme was chosen as a model protein due to its biostability, well-known characteristics, and ease in quantifying its biological activity [39,40]. In addition, its molecular size (14.3 kD) and its basic isoelectric point (around pH = 11) make it an appro-

Table 1
Formulation conditions and protein encapsulation results. **PLGA**, **F68** and **LYS_I** are the initial amount of polymer, surfactant and lysozyme respectively; **Initial%** is the initial polymer-protein rate in w:w; **EE** is the encapsulation efficiency; **LYS_F** is the final encapsulated amount of lysozyme; **DL** is the final drug loading rate in w:w.

	PLGA (mg)	F68 (mg)	LYS_I (mg)	Initial%	EE	LYS_F (mg)	DL
O-F68-Lys	25	15	0.4	1.6	62.5	0.25	1
W-F68-Lys	100	2	0.8	0.8	73.1	0.58	0.58

priate model for other proteins such as bone-growth factors [15]. Three main objectives drove the optimization of the appropriate relation among the polymer, poloxamer, and protein: (1) to have colloidally stable nanosystems of submicron sizes; (2) to encapsulate a sufficient amount of protein; and (3) to prevent protein destabilization by maintaining their biological activity.

Therefore, regardless of the formulation method, it was intended to limit the initial protein loading to provide colloidally stable nanosystems. In our case, as shown in Table 1, Initial% values were the best choice to maintain colloidal stability without significantly changing the size distribution (see below). In consequence, DL presents relative low values for both formulations, although the encapsulated amount of lysozyme, LYS_F, is greater than those required for therapeutic proteins with lower clinically effective amounts [41]. The value of EE found for O-F68-Lys NPs is in consonance with the formulation characteristics and similar to other reports with different proteins [12,10,42,14], including bovine serum albumin (BSA) or insulin [12,42], and several growth factors [14].

The presence of surfactant stabilizes the emulsion droplets and reduces their size. However, it also alters the protein-polymer interaction, which translates into a reduction of the encapsulation efficiency. This was evidenced by Blanco et al. when encapsulating BSA and lysozyme in different PLGA-poloxamer microparticles [10]. Moreover, the type of protein and its initial theoretical loading are factors directly related with the EE and can affect the colloidal stability of the primary emulsion, as shown by Santander et al. [12]. The different polymer:surfactant ratio between the two formulations is not comparable since the surfactant is added in a different way. In both cases, we used previous formulations as the starting point [10,22], and tested several polymer:surfactant ratios (data not shown) in order to obtain the best colloidal stability, EE, and DL. In Table 1 we show the data, for the optimized PLGA:F68 ratios in both systems.

In the W-F68 method, despite the higher EE value with respect to O-F68 system, an almost complete encapsulation was expected, due to the low initial protein:PLGA mass ratio [12] and to the absence of surfactant in the first emulsion step. The characteristics of the modified formulation process may have the key. In this formulation, the relatively high solubility of the ethyl acetate in water promotes rapid diffusion of the organic solvent into the second aqueous phase. An initial small volume of water containing poloxamer is initially added to prevent a rapid, uncontrolled precipitation of the polymer and to control the speed of the process. This is subsequently supplemented with the addition of a larger aqueous volume, as previously described [26]. When this solidification is slow, it favors the escape of the protein and the EE decreases. However, if the solidification is very fast, the contact of protein with the organic solvent is minimized, and the EE increases. On the negative side, it can produce polymer agglomeration, which interferes with the correct formation of the NPs. The introduction of an intermediate step with a reduced volume of aqueous phase with poloxamer can modulate the rate of the process by controlling the diffusion of ethyl acetate into the water and by allowing the diffusion into the organic phase of the poloxamer. A controlled velocity of the polymer pre-solidification process in the presence of surfactant can produce channels or pores in the polymeric shell that, on one hand, could facilitate the protein release and, on the other hand, could drive down the EE value [43]. As a result of these phenomena, the final DLs (w:w of lysozyme:polymer) shown in Table 1 for both NP systems are suitable for their application as nanotransport systems.

3.2. Characterization of the nanoparticles

3.2.1. Interfacial characterization of the first water-in- oil emulsion

To gain better insight into the effect of the formulation method on the interfacial properties of the first water (lysozyme solution)-in-oil emulsion, we designed surface experiments with lysozyme and Pluronic® F68. The main difference in the two formulation methods is how the Pluronic® F68 is added: in aqueous phase (W–F68) or in organic phase (O-F68). This difference could affect the composition of the surface of the NPs and, as a result, their colloidal properties.

The surface tension and elasticity at the air-water interface were the properties analyzed (Table 2). At this interface, proteins change their conformation and expose their hydrophobic part to air, depending on their thermodynamic stability, flexibility, amphipathicity, molecular size, and charge. In our case, lysozyme is a globular protein that is adsorbed at the air-water interface and forms a rigid monolayer due to its internal structure and the presence and number of disulfide bridges [44]. Our measurements were made at pH 12; thus, lysozyme is negatively charged. Table 2 shows the interfacial tension of the lysozyme monolayer at the air-water interface after 50 min of adsorption (45.7 ± 0.4 (mN/m)), and its elasticity (83 ± 4 (mN/m)). The reduction of the interfacial tension when compared with that of the air-water interface (72 mN/m) indicates the surfactant characteristics of the lysozyme. The high value of elasticity was due to the charge and high molecular interactions in the lysozyme monolayer. When the monolayer is formed with Pluronic® F68, the surface tension is slightly lower than with lysozyme when the Pluronic® is added in AP, but similar (taking into account the error) when added in OP.

Pluronic® F68 is an amphiphilic molecule that is adsorbed at the air-water interface when it is dissolved in aqueous phase, and also when it is deposited onto the surface of the drop. Small differences are found when comparing the surface tension of the Pluronic® monolayer from the two methods. The different values of interfacial tension attained in both cases would be due to the different methods to add the Pluronic® F68 at the formed lysozyme monolayer. Pluronic® F68 presents lower elasticity than the lysozyme, as expected since Pluronic® F68 is known to form a flexible monolayer at the air-water interface [45].

Two assays were designed to mimic the formulation methods of the particles. In the first assay, (W-F68 method), a monolayer of lysozyme was formed; then, the bulk of the drop was exchanged with the aqueous solution of Pluronic® F68, and after adsorption the interfacial tension and elasticity of the interface were measured (37.9 ± 0.6 mN/m and 14.2 ± 0.5 mN/m, respectively). This low value of elasticity was very similar to that of the monolayer of Pluronic® F68, indicating that Pluronic® F68 is located at the interface and removes the previously adsorbed lysozyme. In the second assay (O-F68 method) after the monolayer of lysozyme was formed, the Pluronic® F68 dissolved in chloroform is deposited onto the surface of the drop. The chloroform is rapidly evaporated and

Table 2
Interfacial tension and dilatational elasticity (at 1 Hz) of the air-water interface: (a) after adsorbing lysozyme or Pluronic® F68 in the aqueous phase (AP) or Pluronic® F68 in organic phase (OP) in the first step, (b) when Pluronic® F68 is added in AP or OP after adsorption of lysozyme monolayer (mean ± s.d., n = 3).

First step	Interfacial Tension (mN/m)	Elasticity[a] (mN/m)	Second step	Interfacial Tension (mN/m)	Elasticity[b] (mN/m)
Lysozyme	45.7 ± 0.4	83 ± 4	Pluronic® F68 (AP)	37.9 ± 0.6	14.2 ± 0.5
Lysozyme	45.7 ± 0.4	83 ± 4	Pluronic® F68 (OP)	38 ± 2	43 ± 4
Pluronic® F68 (AP)	42.1 ± 0.3	15 ± 3			
Pluronic® F68 (OP)	47.5 ± 2.1	9.4 ± 0.5			

the interfacial tension and elasticity of the interface are measured (38 ± 2 mN/m and 43 ± 4 mN/m, respectively). The elasticity was half of that of the pure lysozyme monolayer, perhaps because of the coexistence of lysozyme and Pluronic® F68 molecules at the interface. The surface tension of the final interface does not depend on the method of adding the Pluronic®, but it is lower than that of the pure lysozyme or the pure Pluronic®.

Within this context, it has been widely reported that the adsorption of PEO and poloxamers at the interface reduces the protein binding [46,47]. In the O-F68 method, the lysozyme is exposed to the DCM after the formation of the first water-in-oil emulsion, even if Pluronic® is added, as they both coexist at the interface. In the W-F68 method, protein will be in contact with ethyl acetate in this step, as Pluronic® is absent. However, this solvent has weaker biological effects on lysozyme. Pluronic® could reach the interface when added to the aqueous phase in the following step, and displace the protein from the interface, which could diffuse outwards to the aqueous phase.

3.2.2. Particle morphology

The delivery, biodistribution, and action mechanism of a transported drug or biomolecule depend heavily on the size of the particle, concentration, and timing [48]. In general, the micrometric scale is designed for a local supply that allows the formation of reservoirs of the transported molecule and minimizes the action of the phagocytic system [49]. However, nanometric systems are more versatile because they permit a systemic distribution, are more stable and reactive and allow extra- as well as intracellular action. This latter mechanism is essential when the molecule or drug should act in the cytoplasm [50] or any other intracellular structure such as the mitochondria, Golgi apparatus, endoplasmic reticulum or nucleus [48,51,52]. Other parameters to alter the intracellular fate of the particles have also been investigated, mainly by altering their surface decoration [53], for example, with nuclear localization signals (NLS) that use the nucleus as the target of the particle [51]. However, these strategies are still in their very early developmental phase [48,52].

A particle size in the submicron scale (between 2 and 500 nm) was sought, as it is necessary for cell internalization and a rapid distribution after parenteral administration in order to reach different tissues through different biological barriers. Particles under 200 nm minimize their intake by macrophages. The type of organic solvent, the polymer concentration, the addition of surfactant, and the emulsification energy control the size of the system.

The O-F68 method gives rise to a monomodal particle-size distribution with diameters around 100 nm. The addition of Pluronic® F68 in the organic phase bolsters colloidal stability of the first emulsion and reduces the particle size in comparison with PLGA NPs, in which the stability is purely electrostatic due to the carboxylic groups of the PLGA. In the W-F68 method, shear stress and volume of the aqueous phase are taken into account to produce a system with particles of between 100 and 500 nm.

O-F68-Lys NPs have a spherical shape with a monomodal size distribution (diameters around 100 nm) and core-shell structure (Fig. 1a). Empty particles produced with the O-F68 method are shown in Figs. S1 (without F68) and S2 (with F68). They are also spherical and with a core-shell structure, but slightly larger.

W-F68-Lys NPs also present a spherical shape but a multimodal size distribution with diameters between 140 and 450 nm, the largest population being around 260 nm (Fig. 1b). A core-shell structure is also observed in these particles. Empty particles from the W-F68 method are presented in Fig. S3, corresponding to a more polydisperse system.

3.2.3. Nanoparticle size, electrokinetic mobility, and colloidal stability

The hydrodynamic diameter distribution of the particles was determined firstly by DLS. Table 3 contains the main colloidal properties of particles produced with the O-F68 and W-F68 methods, empty or loaded with lysozyme. The results of empty particles from the O-F68 method, but synthesized without F68 are also included.

The size parameters were calculated through a cumulative analysis of the data, which is applicable for narrow monomodal size distributions [34]. SEM and STEM micrographs indicate that such an approximation could be assumed for particles from the O-F68 method, but not from the W-F68 one. Thus, the intensity size distributions of the different systems are shown in Fig. 2a. The presence of Pluronic® F68 in the O-F68 method significantly reduces the size and polydispersity of the NPs. This agrees with the reduction of the surface tension when the F68 is at the interface (Table 2), which promotes the emulsification process. If the NPs are also loaded with lysozyme, the size is even smaller, but the polydispersity increases slightly compared with the empty particles. The surfactant properties of the lysozyme have been shown with the surface-tension results (Table 2).

Fig. 2a indicates the presence of particles higher than 500 nm with the W-F68, which does not correlate with the SEM micrographs. Thus, a different technique (NTA) was used to gain information on the size distribution of such systems (Fig. 3b). With NTA, the size distribution was consistent with the SEM images. Broad size distributions corresponding to multimodal systems were found with this method, but the addition of lysozyme led to a clear size reduction. This is because lysozyme also acts as an emulsifier in the first emulsion.

The electrokinetic charge of the NPs was analyzed by measuring the electrophoretic mobility. For comparison, all the samples were measured at pH 7 (phosphate buffer). In Fig. 3, the electrophoretic mobility distributions are presented while the corresponding μ-averages are shown in Table 3.

PLGA NPs are usually negatively charged due to the carboxylic groups of the polymer. The use of Pluronic® F68 in the O-F68 method clearly reduces the electrophoretic mobility of the NPs, which indicates that some Pluronic® is located at the NP surface. This reduction was expected after the incorporation of this non-ionic surfactant onto the interface, since the presence of polyethylene oxide chains would cause an outward shift of the shear plane where the ζ-potential is defined, and this would subsequently diminish electrophoretic mobility. Previous results for PLGA particles have shown a significant reduction directly related to the poloxamer coating [54]. If we compare the two systems, the

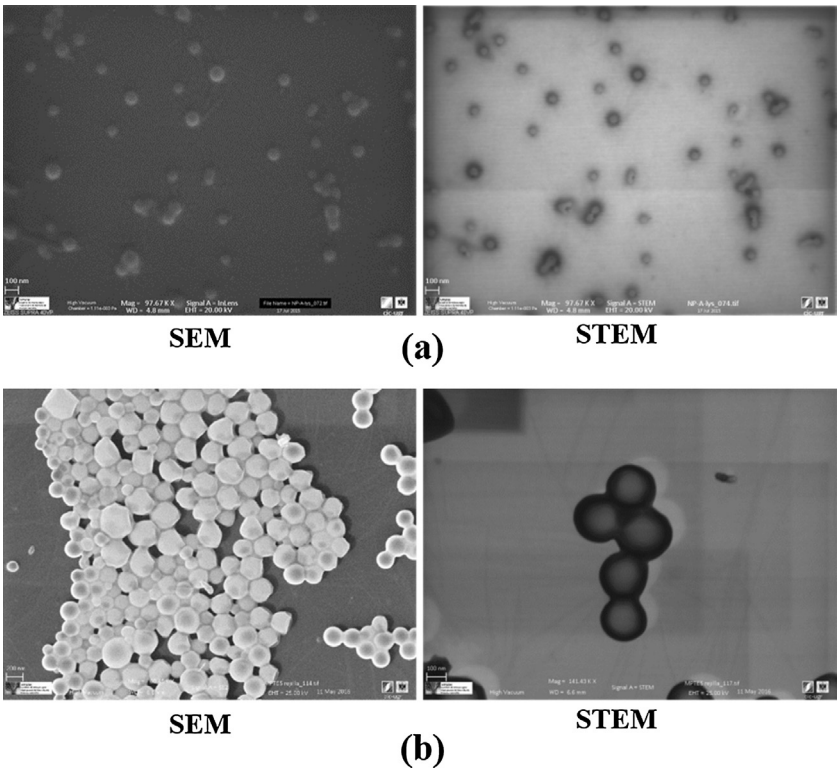

Fig. 1. SEM and STEM micrographs of lysozyme-loaded particles using O-F68 (a) or W-F68 method (b).

Table 3
Colloidal properties of PLGA NPs from different formulation methods. They were measured in phosphate buffer (pH 7). The average hydrodynamic diameter (Z-average or cumulative mean) and the polydispersity index (PDI) are determined from DLS. (Mean ± s.d., n = 3).

		Z-average (nm)	PDI	μ-average (μmcm/Vs)
O-F68 method	Empty, without F68	266 ± 7	0.293	−5.06 ± 0.15
	Empty	162.7 ± 2.1	0.081	−4.29 ± 0.18
	Lysozyme-loaded	121.0 ± 1.2	0.244	−3.34 ± 0.07
W-F68 method	Empty	273 ± 3	0.193	−5.31 ± 0.11
	Lysozyme-loaded	293 ± 4	0.169	−4.212 ± 0.013

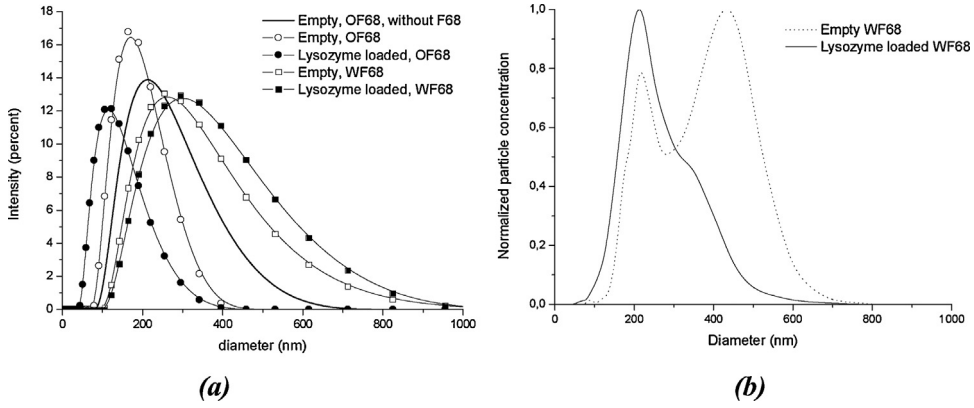

Fig. 2. Hydrodynamic diameter distribution, **(a)** by DLS at pH 7 (phosphate buffer) of empty and lysozyme-loaded PLGA particles from the O-F68 and W-F68 methods; and **(b)** by NTA at pH 7 (phosphate buffer) of empty and lysozyme-loaded PLGA particles from the W-F68 method.

less negative surface for OF68 NPs would be related to less density of surface PLGA polymer, bringing the negative electrical charge to the interface. This result would be in line with the greater amount of PLGA in the formulation of WF68 nanosystem.

When the lysozyme is also used in the synthesis, the surface is even less negative, which could be explained by the presence of some protein (whose net charge is positive) near or at the interface. This latter effect is also found with the W-F68 method. The attractive electrostatic interaction between negative terminal acid residues of PLGA and lysozyme molecules plays a key role in the process of protein encapsulation [41] or adsorption [40] in PLGA NPs, which affects the final protein loading. In relation

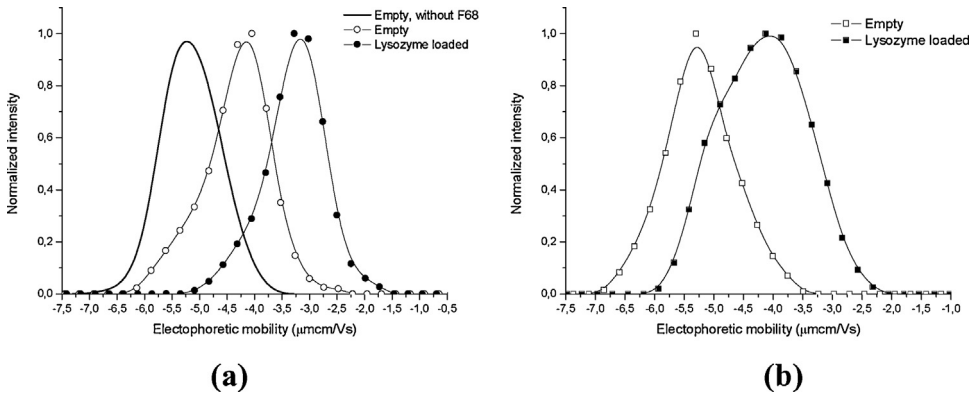

Fig. 3. Electrophoretic mobility distribution at pH 7 (phosphate buffer) of empty and lysozyme-loaded PLGA particles from the (a) O-F68 and (b) W-F68 methods.

to this situation, an important characteristic of the W-F68 encapsulation formulation is that the water phase is at pH 12, which allows a negative net charge of lysozyme and, thus, avoids the electrostatic protein-polymer attraction. This situation can reduce the encapsulation efficiency but at the same time favors the later protein-diffusion process and consequently the short-term release.

Recent studies have proposed the use of nanoparticles embedded in predesigned 3D-printed scaffolds [55,56], moving us to analyze the stability of the two formulations in several media usually employed during the preparation of other structures. Size distributions similar to the original were found for the two formulations in different media (PB, PBS, and DMEM) and at different times after synthesis (0, 1, and 5 days). The electric charge of PLGA acid end groups and the poloxamer molecules located on the NP surface confers a combined electrostatic and steric, colloidal-stability mechanism, as has previously been described [46,54]. Additionally, the NPs in all cases keep their size under storage at 4 °C at least for 1 month (data not shown). Thus, the media described could potentially be used as storage media or to prepare other solutions or scaffolds before actually placing them in the living environment (*in vitro* or *in vivo*).

3.2.4. NMR of the nanoparticles

In Fig. 3, both empty and protein-loaded NPs present less negative electrophoretic mobility than do empty NPs without F68, which could be explained by the presence of Pluronic® F68 at the surface of the NP. By comparing the 1HNMR spectra of free Pluronic® F68, and lysozyme-loaded NPs from O-F68 and W-F68 methods, we can check the presence of F68 at the surface of the NPs (Fig. S4) by the peaks shown between 3.25 and 3.75 ppm and at 1 ppm. These peaks are also visible in the spectra of NPs formulated with F68 (O-F68 and W-F68, Figs. S5, and S6, respectively).

3.3. Biological activity and interactions

A controlled release from a PLGA-based delivery system is a difficult task, as it depends on multiple factors: the type of PLGA, solvent, mechanical stress, use of surfactants, etc. [57]. The diffusion of the protein and the polymer erosion are the main mechanisms involved in the protein release in PLGA-based delivery systems. Furthermore, it is typical to find a rapid burst release at the initial stage, followed by a slow release phase, over the short and medium term. In this phase, protein molecules diffuse through the polymer matrix until reaching a final phase in which the polymer degradation by hydrolysis allows a faster release [20].

On the other hand, the short-term release is of special interest for transporting bone morphogenetic growth factors (BMPs). A controlled initial burst followed by a sustained release significantly improves *in vivo* regeneration of bone [3] and cartilage [58] even in dual-controlled release systems [59]. For these reasons, we focused our analysis on short-term release, taking into account the reduced polymer degradation by hydrolysis found for similar systems for these early steps [60].

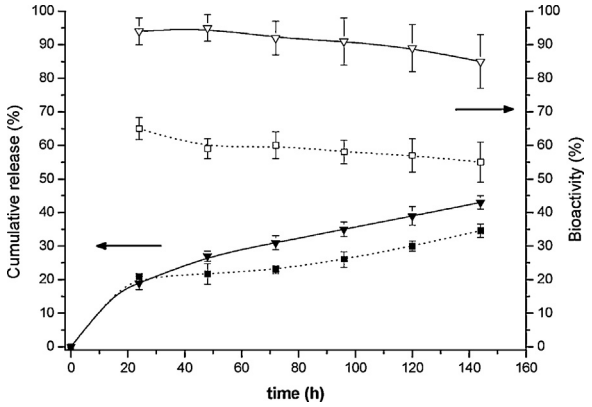

Fig. 4. Cumulative release (filled symbols) and residual bioactivity (open symbols) of O-F68-Lys (square) and W-F68-Lys (triangle) incubated for different times at 37 °C in saline phosphate buffer (pH 7.4) (mean ± s.d, n = 3).

Fig. 4 shows the accumulative release of lysozyme from O-F68-Lys NPs over the short term (seven days). These results are consistent with a two-stepped process: an initial burst and a slow-release phase. The first step could correspond to the release of the protein molecules located near surface, whose presence was deduced from the electrophoretic mobility results (Fig. 3). The second part of the release process was limited and slow due to the protein diffusion through the matrix of the polymeric shell. The specific electrostatic interaction between the positive lysozyme molecules and the PLGA negative terminal acid groups can reduce the protein diffusion [10]. When the poloxamer (F68) is added, the interaction between the surfactant and the protein helps the diffusion process, leading to a more complete and sustained release [12]. It also helps to keep the biological activity of the protein [41,61]. The poloxamer reduces the non-specific protein-polymer interactions (i.e. hydrophobic interactions) but not the specific ones (electrostatics); thus, the diffusion through water-filled pores or through the polymer is still limited. In the current study, the protein fraction released and the release pattern are similar to those found in the literature for lysozyme encapsulated in nano- and microparticles of blends of PLGA and other polymers or surfactants [26,15,11].

The protein release curve from W-F68-Lys NPs (Fig. 4) reveals that the initial delivery rate is identical to that of the O-F68 system, which could mean a similar proportion of encapsulated protein close to or at the surface for both NP systems. This would agree with the analogous decrease in the electrophoretic mobility of the

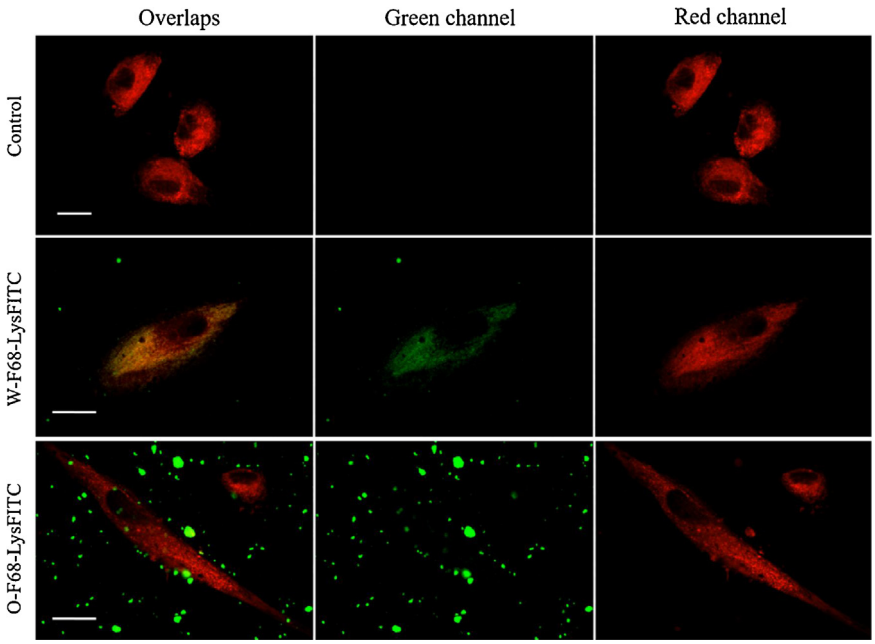

Fig. 5. z-projection of 5 images of hMSCs visualized 30 min after incubation with W-F68-LysFITC NPs or O-F68-LysFITC NPs. hMSCs were previously labeled with cell-tracker red. Scale bar 20 μm.

lysozyme-loaded NPs previously reported (Fig. 3). In the second part of the process, the specific interaction between the protein and the polymer is again present. However, the diffusion process in the W-F68 system appears to be enhanced, allowing a continuous and sustained release after the initial burst and reaching a slightly higher value for the maximum release time studied. This result could be related to the inner structure of the polymer layer that allows better hydration and, therefore, better diffusion of the protein towards the outside. It has been previously reported that the use of less polar organic solvents, such as DCM, for PLGA particles formulations increases the density of the polymer matrix in comparison with more polar organic solvents such as EA. The PLGA matrices prove more resistant in the first case, but reducing at the same time their connectivity and diffusivity [62]. Meng et al. [26] found that faster removal of EA results in a slower kinetic release of the protein due to a decrease in the porosity of the NPs. Regarding the role of the Pluronic®, Rafati et al. [63] found a higher concentration of protein encapsulated in the surface pores in microparticles synthesized in the presence of surfactant in the second aqueous phase of the emulsion. Since an intermediate step was introduced in our W-F68 formulation in the second aqueous phase of the emulsion, the removal of the EA by diffusion was strongly controlled, so that it was expected that the porosity of these NPs would increase. This porosity improves protein diffusion, which allows a more stable release pattern according to the experimental result found for this system. Despite the unfavorable effect of the specific electrostatic protein-polymer interaction on the release, the amount of released protein in our NPs is substantial, signifying that there are other unspecific interactions that can be modulated by the presence of surfactant allowing a sustained release. The amount of released lysozyme is similar to that found with lysozyme physically adsorbed onto the surface of PLGA nanoparticles despite the electrostatic attraction [40]. Besides other unspecific interactions, the electrolyte concentration in the release medium could modulate this electrostatic attraction between the protein and polymer, diminishing it and facilitating the release process [46].

Another remarkable parameter is the biological activity of the *in vitro* release of lysozyme shown in Fig. 4. While in the O-F68 system the bioactivity is partially reduced by up to 40%, the protein supplied by the W-F68 system maintains the activity above 90% with respect to that of commercially supplied lysozyme and resuspended in the same release buffer. As discussed above, both the organic solvent and the hydrophobic interaction between the protein and the polymer often cause denaturation of encapsulated proteins [41,64]. Perez et al. [11] describe a partial loss of activity when using DCM and an aqueous PVA solution in the second emulsification step without any additional excipient. The use of poloxamers in the formulation reduces such interactions, enhances the stability of the protein, and maintains an aqueous layer that retains the water molecules necessary for the biological function of the protein, at the same time aiding its diffusion. This situation, together with the use of a weak organic solvent such as EA, helps preserve the biological activity of the lysozyme, as found for the W-F68-Lys system.

Fig. S7 presents different confocal microscopy images related to the release process of lysozyme-loaded W-F68 NPs. A decrease in fluorescence intensity was appreciable over the course of the *in vitro* experiment. In addition, the aggregation of the system is visible as the incubation process progresses. The analysis of these images is consistent with the previously reported results for this NP system.

3.3.1. Cellular uptake

Cellular uptake of PLGA NPs is a known process affected mainly by surface properties and functionalization [9] and particle aggregation [65]. Internalization and subsequent intracellular processing of the particles have been described as an active process; thus, it is energy dependent and can, therefore, be affected by other factors that alter the energy uptake by cells, such as temperature [48]. Particles can be internalized by several endocytosis methods, dependent primarily on the size of the particle: caveolin-dependent particles (diameter ≈ 60 nm), clathrin-independent (diameter ≈ 90 nm) and clathrin-dependent (diameter ≈ 120 nm) [51,52]. Once internalized, about 65% are exported back to the extracellular space before releasing any of their content, while the rest slowly release the encapsulated molecule into the intracellular space [66]. The intracellular release process is affected by the formulation of the particles [48]. We have

demonstrated that the proposed systems follow a pattern similar to others previously published. As early as 30 min after incubation, W-F68-LysFITC NPs were taken up by the cells (Fig. 5). Some W-F68 particles were still in the medium so that the dual activity could happen. In contrast, O-F68-LysFITC NPs were affected by aggregation and, therefore, did not properly reach the intracellular space (Fig. 5; for z-axis images view Fig. S8). This contradicts the previous analyses of the colloidal stability in PB, PBS and DMEM. This finding can be explained by the fact that although the culture media was DMEM, this latter medium was supplemented with fetal bovine serum, and cells release many factors to the extracellular medium that can affect these types of particles. None of the systems were shown to be toxic for the cells (Fig. S9). No studies available have reported any effects of lysozyme on hMSCs.

4. Conclusions

A novel dual-delivery PLGA-nanosystem has been developed in which the formulation and components favor an adequate short-term delivery pattern while preserving the bioactivity of encapsulated molecules. The analysis of the polymer-surfactant-protein interaction shows that the organic solvent, use of surfactant, volume relation of both phases, and the net charge of the protein play important roles in the final characteristics and release behavior of the nanoparticles. The W-F68 formulation balances all of them in order to provide a nanosystem ready to transport and deliver hydrophilic biomolecules such as proteins. *In vitro* release experiments display an adequate short-term delivery pattern that at the same time preserves the bioactivity of the encapsulated biomolecule. Additionally, the singular nanoparticle size distribution found for this W-F68 nanosystem allows the possibility of a dual, outer-, and intra-cellular, protein delivery as has been shown by *in vitro* cellular experiments. This novel formulation will be used in future studies to encapsulate and deliver growth factors *in vitro* and *in vivo* in order to exploit the therapeutic potential of this nanosystem.

Acknowledgements

The authors wish to express their appreciation for the technical support to Dr. Azahara Rata-Aguilar and for the financial support granted by the Consejería de Economía, Innovación, Ciencia y Empleo de la Junta de Andalucía (Spain) through research groups FQM-115 and CTS-1028 and by the following research project: MAT2013-43922-R – European FEDER support included – (MICINN, Spain).

Appendix A. Supplementary data

Supplementary data associated with this article can be found, in the online version, at http://dx.doi.org/10.1016/j.colsurfb.2017.08.027.

References

[1] M. Padial-Molina, J.T. Marchesan, A.D. Taut, Q. Jin, W.V. Giannobile, H.F. Rios, Methods to Validate Tooth-supporting Regenerative Therapies, 2012, http://dx.doi.org/10.1007/978-1-61779-860-3_13.
[2] M. Padial-Molina, J.C. Rodriguez, S.L. Volk, H.F. Rios, Standardized in vivo model for studying novel regenerative approaches for multitissue bone-ligament interfaces, Nat. Protoc. 10 (2015), http://dx.doi.org/10.1038/nprot.2015.063.
[3] Bone regeneration from PLGA micro-Nanoparticles, Biomed Res. Int. (2015) http://www.hindawi.com/journals/bmri/aa/415289/.
[4] K.-B. Lee, A. Solanki, J. Kim, J. Jung, Nanomedicine: dynamic integration of nanotechnology with biomedical science, in: Handb. Clin. Nanomedicine, Pan Stanford, 2016, 2017, pp. 21–60, http://dx.doi.org/10.1201/b19915-4.
[5] G.E.J. Poinern, A Laboratory Course in Nanoscience and Nanotechnology, CRC, Press Taylor & Francis Group, 2015.
[6] M.M. Yallapu, B.K. Gupta, M. Jaggi, S.C. Chauhan, Fabrication of curcumin encapsulated PLGA nanoparticles for improved therapeutic effects in metastatic cancer cells, J. Colloid Interface Sci. 351 (2010) 19–29, http://dx.doi.org/10.1016/j.jcis.2010.05.022.
[7] B.P. Nair, C.P. Sharma, Poly(lactide-co-glycolide)-laponite-F68 nanocomposite vesicles through a single-step double-emulsion method for the controlled release of doxorubicin, Langmuir 28 (2012) 4559–4564, http://dx.doi.org/10.1021/la300005c.
[8] R. Shankarayan, S. Kumar, P. Mishra, Differential permeation of piroxicam-loaded PLGA micro/nanoparticles and their in vitro enhancement, J. Nanopart. Res. 15 (2013) 1496, http://dx.doi.org/10.1007/s11051-013-1496-6.
[9] J.A. Loureiro, B. Gomes, G. Fricker, M.A.N. Coelho, S. Rocha, M.C. Pereira, Cellular uptake of PLGA nanoparticles targeted with anti-amyloid and anti-transferrin receptor antibodies for Alzheimer's disease treatment, Colloids Surf. B Biointerfaces 145 (2016) 8–13, http://dx.doi.org/10.1016/j.colsurfb.2016.04.041.
[10] D. Blanco, M.J. Alonso, Protein encapsulation and release from poly(lactide-co-glycolide) microspheres: effect of the protein and polymer properties and of the co- encapsulation of surfactants, Eur. J. Pharm. Biopharm. 45 (1998) 285–294, http://dx.doi.org/10.1016/S0939-6411(98)00011-3.
[11] C. Pérez, P. De Jesús, K. Griebenow, Preservation of lysozyme structure and function upon encapsulation and release from poly(lactic-co-glycolic) acid microspheres prepared by the water-in-oil-in-water method, Int. J. Pharm. 248 (2002) 193–206, http://dx.doi.org/10.1016/S0378-5173(02)00435-0.
[12] M.J. Santander-Ortega, N. Csaba, L. González, D. Bastos-González, J.L. Ortega-Vinuesa, M.J. Alonso, Protein-loaded PLGA–PEO blend nanoparticles: encapsulation, release and degradation characteristics, Colloid. Polym. Sci. 288 (2010) 141–150, http://dx.doi.org/10.1007/s00396-009-2131-z.
[13] N. Pirooznia, S. Hasannia, A. Lotfi, M. Ghanei, Encapsulation of alpha-1 antitrypsin in PLGA nanoparticles: in Vitro characterization as an effective aerosol formulation in pulmonary diseases, J. Nanobiotechnol. 10 (2012) 20, http://dx.doi.org/10.1186/1477-3155-10-20.
[14] I. D'Angelo, M. Garcia-Fuentes, Y. Parajó, A. Welle, T. Vántus, A. Horváth, G. Bökönyi, G. Kéri, M.J. Alonso, Nanoparticles based on PLGA: poloxamer blends for the delivery of proangiogenic growth factors, Mol. Pharm. 7 (2010) 1724–1733, http://dx.doi.org/10.1021/mp1001262.
[15] L.J. White, G.T.S. Kirby, H.C. Cox, R. Qodratnama, O. Qutachi, F.R.A.J. Rose, K.M. Shakesheff, Accelerating protein release from microparticles for regenerative medicine applications, Mater. Sci. Eng. C 23 (2013) 2578–2583, http://dx.doi.org/10.1016/j.msec.2013.02.020.
[16] P. Pantazis, K. Dimas, J.H. Wyche, S. Anant, C.W. Houchen, J. Panyam, R.P. Ramanujam, Preparation of siRNA-Encapsulated PLGA nanoparticles for sustained release of siRNA and evaluation of encapsulation efficiency, Nanopart. Biol. Med. (2012) 311–319, http://dx.doi.org/10.1007/978-1-61779-953-2_25, Humana Press, Totowa, NJ.
[17] J.S. Park, H.N. Yang, D.G. Woo, S.Y. Jeon, K.H. Park, Multilineage differentiation of human-derived dermal fibroblasts transfected with genes coated on PLGA nanoparticles plus growth factors, Biomaterials 34 (2013) 582–597, http://dx.doi.org/10.1016/j.biomaterials.2012.10.001.
[18] F. Wan, M. Yang, Design of PLGA-based depot delivery systems for biopharmaceuticals prepared by spray drying, Int. J. Pharm. 498 (2016) 82–95, http://dx.doi.org/10.1016/j.ijpharm.2015.12.025.
[19] A. Giteau, M.C. Venier-Julienne, A. Aubert-Pouëssel, J.P. Benoit, How to achieve sustained and complete protein release from PLGA-based microparticles? Int. J. Pharm. 350 (2008) 14–26, http://dx.doi.org/10.1016/j.ijpharm.2007.11.012.
[20] S. Fredenberg, M. Wahlgren, M. Reslow, A. Axelsson, The mechanisms of drug release in poly(lactic-co-glycolic acid)-based drug delivery systems—a review, Int. J. Pharm. 415 (2011) 34–52, http://dx.doi.org/10.1016/j.ijpharm.2011.05.049.
[21] F. Mohamed, C.F. van der Walle, Engineering biodegradable polyester particles with specific drug targeting and drug release properties, J. Pharm. Sci. 97 (2008) 71–87, http://dx.doi.org/10.1002/jps.21082.
[22] N. Csaba, L. González, A. Sánchez, M.J. Alonso, Design and characterisation of new nanoparticulate polymer blends for drug delivery, J. Biomater. Sci. Polym. Ed. 15 (2004) 1137–1151, http://dx.doi.org/10.1163/1568562041753098.
[23] H.K. Makadia, S.J. Siegel, Poly lactic-co-glycolic acid (PLGA) as biodegradable controlled drug delivery carrier, Polymers (Basel) 3 (2011) 1377–1397, http://dx.doi.org/10.3390/polym3031377.
[24] F. Danhier, E. Ansorena, J.M. Silva, R. Coco, A. Le Breton, V. Préat, PLGA-based nanoparticles: an overview of biomedical applications, J. Controlled Release 161 (2012) 505–522, http://dx.doi.org/10.1016/j.jconrel.2012.01.043.
[25] G. Ratzinger, U. Länger, L. Neutsch, F. Pittner, M. Wirth, F. Gabor, Surface modification of PLGA particles: the interplay between stabilizer, ligand size, and hydrophobic interactions, Langmuir 26 (2010) 1855–1859, http://dx.doi.org/10.1021/la902602z.
[26] F.T. Meng, G.H. Ma, W. Qiu, Z.G. Su, W/O/W double emulsion technique using ethyl acetate as organic solvent: effects of its diffusion rate on the characteristics of microparticles, J. Controlled Release 91 (2003) 407–416, http://dx.doi.org/10.1016/S0168-3659(03)00273-6.
[27] M. Padial-Molina, F. O'Valle, A. Lanis, F. Mesa, D.M. Dohan Ehrenfest, H.-L. Wang, P. Galindo-Moreno, Clinical application of mesenchymal stem cells and novel supportive therapies for oral bone regeneration, Biomed. Res. Int. 2015 (2015), http://dx.doi.org/10.1155/2015/341327.

[28] P. Yilgor, N. Hasirci, V. Hasirci, Sequential BMP-2/BMP-7 delivery from polyester nanocapsules, J. Biomed. Mater. Res. – Part A 93 (2010) 528–536, http://dx.doi.org/10.1002/jbm.a.32520.
[29] B. Li, T. Yoshii, A.E. Hafeman, J.S. Nyman, J.C. Wenke, S.A. Guelcher, The effects of rhBMP-2 released from biodegradable polyurethane/microsphere composite scaffolds on new bone formation in rat femora, Biomaterials 30 (2009) 6768–6779, http://dx.doi.org/10.1016/j.biomaterials.2009.08.038.
[30] Y. Wang, Y. Wei, X. Zhang, M. Xu, F. Liu, Q. Ma, Q. Cai, X. Deng, PLGA/PDLLA core-shell submicron spheres sequential release system: preparation, characterization and promotion of bone regeneration in vitro and in vivo, Chem. Eng. J. 273 (2015) 490–501, http://dx.doi.org/10.1016/j.cej.2015.03.068.
[31] Y.B. Shim, H.H. Jung, J.W. Jang, H.S. Yang, H. Bae, J.C. Park, B. Choi, S.H. Lee, Fabrication of hollow porous PLGA microspheres using sucrose for controlled dual delivery of dexamethasone and BMP2, J. Ind. Eng. Chem. 37 (2016) 101–106, http://dx.doi.org/10.1016/j.jiec.2016.03.014.
[32] J. Maldonado-Valderrama, J.A.H. Terriza, A. Torcello-Gómez, M.A. Cabrerizo-Vílchez, In vitro digestion of interfacial protein structures, Soft Matter (2013) 1043–1053, http://dx.doi.org/10.1039/c2sm26843d.
[33] M. a Cabrerizo-Vilchez, H. a Wege, J. a Holgado-Terriza, a W. Neumann, Axisymmetric drop shape analysis as penetration Langmuir balance, Rev. Sci. Instrum. 70 (1999) 2438–2444, http://dx.doi.org/10.1063/1.1149773.
[34] P.A. Hassan, S. Rana, G. Verma, Making sense of brownian motion: colloid characterization by dynamic light scattering, Langmuir 31 (2015) 3–12, http://dx.doi.org/10.1021/la501789z.
[35] R.J. Kok, M. Haas, F. Moolenaar, D. de Zeeuw, D.K. Meijer, Drug delivery to the kidneys and the bladder with the low molecular weight protein lysozyme, Ren. Fail. 20 (1998) 211–217.
[36] S. Mason, S.A. Tarle, W. Osibin, Y. Kinfu, D. Kaigler, Standardization and safety of alveolar bone-derived stem cell isolation, J. Dent. Res. 93 (2014) 55–61, http://dx.doi.org/10.1177/0022034513510530.
[37] C. Farace, P. Sánchez-Moreno, M. Orecchioni, R. Manetti, F. Sgarrella, Y. Asara, J.M. Peula-García, J.A. Marchal, R. Madeddu, L.G. Delogu, Immune cell impact of three differently coated lipid nanocapsules: pluronic, chitosan and polyethylene glycol, Sci. Rep. 6 (2016) 18423, http://dx.doi.org/10.1038/srep18423.
[38] C. Sturesson, J. Carlfors, Incorporation of protein in PLG-microspheres with retention of bioactivity, J. Controlled Release 67 (2000) 171–178, http://dx.doi.org/10.1016/S0168-3659(00)00205-4.
[39] L. Ying, S. Jiali, J. Guoqiang, Z. Jia, D. Fuxin, In vitro evaluation of lysozyme-loaded microspheres in thermosen- sitive methylcellulose-based hydrogel, Chin. J. Chem. Eng. 15 (2007) 566–572.
[40] C. Cai, U. Bakowsky, E. Rytting, A.K. Schaper, T. Kissel, Charged nanoparticles as protein delivery systems: a feasibility study using lysozyme as model protein, Eur. J. Pharm. Biopharm. 69 (2008) 31–42, http://dx.doi.org/10.1016/j.ejpb.2007.10.005.
[41] A. Paillard-Giteau, V.T. Tran, O. Thomas, X. Garric, J. Coudane, S. Marchal, I. Chourpa, J.P. Benoît, C.N. Montero-Menei, M.C. Venier-Julienne, Effect of various additives and polymers on lysozyme release from PLGA microspheres prepared by an s/o/w emulsion technique, Eur. J. Pharm. Biopharm. 75 (2010) 128–136, http://dx.doi.org/10.1016/j.ejpb.2010.03.005.
[42] M.J. Santander-Ortega, D. Bastos-González, J.L. Ortega-Vinuesa, M.J. Alonso, Insulin-loaded PLGA nanoparticles for oral administration: an *in vitro* physico-chemical characterization, J. Biomed. Nanotechnol. 5 (2009) 45–53, http://dx.doi.org/10.1166/jbn.2009.022.
[43] I.D. Rosca, F. Watari, M. Uo, Microparticle formation and its mechanism in single and double emulsion solvent evaporation, J. Controlled Release 99 (2004) 271–280, http://dx.doi.org/10.1016/j.jconrel.2004.07.007.
[44] S. Pezennec, F. Gauthier, C. Alonso, F. Graner, T. Croguennec, G. Brulé, A. Renault, The protein net electric charge determines the surface rheological properties of ovalbumin adsorbed at the air-water interface, Food Hydrocolloids 14 (2000) 463–472, http://dx.doi.org/10.1016/S0268-005X(00)00026-6.
[45] A. Torcello-Gómez, M.J. Santander-Ortega, J.M. Peula-García, J. Maldonado-Valderrama, M.J. Gálvez-Ruiz, J.L. Ortega-Vinuesa, A. Martín-Rodríguez, Adsorption of antibody onto pluronic F68-covered nanoparticles: link with surface properties, Soft Matter 7 (2011) 8450, http://dx.doi.org/10.1039/c1sm05570d.
[46] M.J. Santander-Ortega, M.V. Lozano-López, D. Bastos-González, J.M. Peula-García, J.L. Ortega-Vinuesa, Novel core-shell lipid-chitosan and lipid-poloxamer nanocapsules: stability by hydration forces, Colloid. Polym. Sci. 288 (2010) 159–172, http://dx.doi.org/10.1007/s00396-009-2132-y.
[47] A. Torcello-Gómez, M.J. Santander-Ortega, J.M. Peula-García, J. Maldonado-Valderrama, M.J. Gálvez-Ruiz, J.L. Ortega-Vinuesa, A. Martín-Rodríguez, Adsorption of antibody onto Pluronic F68-covered nanoparticles: link with surface properties, Soft Matter 7 (2011), http://dx.doi.org/10.1039/c1sm05570d.
[48] J.P. Peñaloza, V. Márquez-Miranda, M. Cabaña-Brunod, R. Reyes-Ramírez, F.M. Llancalahuen, C. Vilos, F. Maldonado-Biermann, L.A. Velásquez, J.A. Fuentes, F.D. González-Nilo, M. Rodríguez-Díaz, C. Otero, Intracellular trafficking and cellular uptake mechanism of PHBV nanoparticles for targeted delivery in epithelial cell lines, J. Nanobiotechnol. 15 (2017) 1, http://dx.doi.org/10.1186/s12951-016-0241-6.
[49] S.P. Schwendeman, R.B. Shah, B.A. Bailey, A.S. Schwendeman, Injectable controlled release depots for large molecules, J. Controlled Release 190 (2014) 240–253, http://dx.doi.org/10.1016/j.jconrel.2014.05.057.
[50] H. Wang, S.C.G. Leeuwenburgh, Y. Li, J.A. Jansen, The use of micro- and nanospheres as functional components for bone tissue regeneration, Tissue Eng. Part B Rev. 18 (2012) 24–39, http://dx.doi.org/10.1089/ten.teb.2011.0184.
[51] J.K. Vasir, V. Labhasetwar, Biodegradable nanoparticles for cytosolic delivery of therapeutics, Adv. Drug Deliv. Rev. 59 (2007) 718–728, http://dx.doi.org/10.1016/j.addr.2007.06.003.
[52] B. Yameen, W. Il Choi, C. Vilos, A. Swami, J. Shi, O.C. Farokhzad, Insight into nanoparticle cellular uptake and intracellular targeting, J. Controlled Release 190 (2014) 485–499, http://dx.doi.org/10.1016/j.jconrel.2014.06.038.
[53] H. Sneh-Edri, D. Likhtenshtein, D. Stepensky, Intracellular targeting of PLGA nanoparticles encapsulating antigenic peptide to the endoplasmic reticulum of dendritic cells and its effect on antigen cross-presentation in vitro, Mol. Pharm. 8 (2011) 1266–1275, http://dx.doi.org/10.1021/mp200198c.
[54] M.J. Santander-Ortega, A.B. Jódar-Reyes, N. Csaba, D. Bastos-González, J.L. Ortega-Vinuesa, Colloidal stability of Pluronic F68-coated PLGA nanoparticles: a variety of stabilisation mechanisms, J. Colloid Interface Sci. 302 (2006) 522–529, http://dx.doi.org/10.1016/j.jcis.2006.07.031.
[55] B. Baumann, T. Jungst, S. Stichler, S. Feineis, O. Wiltschka, M. Kuhlmann, M. Lind??n, J. Groll, Control of nanoparticle release kinetics from 3D printed hydrogel scaffolds, Angew. Chem. – Int. Ed. 56 (2017) 4623–4628, http://dx.doi.org/10.1002/anie.201700153.
[56] S.-J. Lee, W. Zhu, L. Heyburn, M. Nowicki, B. Harris, L.G. Zhang, Development of novel 3-D printed scaffolds with core-shell nanoparticles for nerve regeneration, IEEE Trans. Biomed. Eng. 64 (2017) 408–418, http://dx.doi.org/10.1109/tbme.2016.2558493.
[57] D.J. Hines, D.L. Kaplan, Poly(lactic-co-glycolic) acid-controlled-release systems: experimental and modeling insights, Crit. Rev. Ther. Drug Carrier Syst. 30 (2013) 257–276, http://dx.doi.org/10.1615/CritRevTherDrugCarrierSyst.2013006475.
[58] H. Begam, S.K. Nandi, B. Kundu, A. Chanda, Strategies for delivering bone morphogenetic protein for bone healing, Mater. Sci. Eng. C 70 (2016) 856–869, http://dx.doi.org/10.1016/j.msec.2016.09.074.
[59] Y.H. Kim, Y. Tabata, Dual-controlled release system of drugs for bone regeneration, Adv. Drug Deliv. Rev. 94 (2015) 28–40, http://dx.doi.org/10.1016/j.addr.2015.06.003.
[60] N. Rescignano, L. Tarpani, A. Romani, I. Bicchi, S. Mattioli, C. Emiliani, L. Torre, J.M. Kenny, S. Martino, L. Latterini, I. Armentano, In-vitro degradation of PLGA nanoparticles in aqueous medium and in stem cell cultures by monitoring the cargo fluorescence spectrum, Polym. Degrad. Stab. 134 (2016) 296–304, http://dx.doi.org/10.1016/j.polymdegradstab.2016.10.017.
[61] M. Morille, T. Van-Thanh, X. Garric, J. Cayon, J. Coudane, D. Noël, M.C. Venier-Julienne, C.N. Montero-Menei, New PLGA-P188-PLGA matrix enhances TGF-β3 release from pharmacologically active microcarriers and promotes chondrogenesis of mesenchymal stem cells, J. Control. Release. 170 (2013) 99–110, http://dx.doi.org/10.1016/j.jconrel.2013.04.017.
[62] A. Bohr, F. Wan, J. Kristensen, M. Dyas, E. Stride, S. Baldursdottír, M. Edirisinghe, M. Yang, Pharmaceutical microparticle engineering with electrospraying: the role of mixed solvent systems in particle formation and characteristics, J. Mater. Sci. Mater. Med. 26 (2015) 61, http://dx.doi.org/10.1007/s10856-015-5379-5.
[63] A. Rafati, A. Boussahel, K.M. Shakesheff, A.G. Shard, C.J. Roberts, X. Chen, D.J. Scurr, S. Rigby-Singleton, P. Whiteside, M.R. Alexander, M.C. Davies, Chemical and spatial analysis of protein loaded PLGA microspheres for drug delivery applications, J. Control. Release. 162 (2012) 321–329, http://dx.doi.org/10.1016/j.jconrel.2012.05.008.
[64] R. Gaudana, M. Gokulgandhi, V. Khurana, D. Kwatra, A.K. Mitra, Design and evaluation of a novel nanoparticulate-based formulation encapsulating a HIP complex of lysozyme, Pharm. Dev. Technol. 18 (2013) 752–759, http://dx.doi.org/10.3109/10837450.2012.737806.
[65] S. Xiong, X. Zhao, B.C. Heng, K.W. Ng, J.S.C. Loo, Cellular uptake of Poly-(D, L-lactide-co-glycolide) (PLGA) nanoparticles synthesized through solvent emulsion evaporation and nanoprecipitation method, Biotechnol. J. 6 (2011) 501–508, http://dx.doi.org/10.1002/biot.201000351.
[66] J. Panyam, V. Labhasetwar, Dynamics of endocytosis and exocytosis of poly (D, L-lactide-co-glycolide) nanoparticles in vascular smooth muscle cells, Pharm. Res. 20 (2003) 212–220 http://www.ncbi.nlm.nih.gov/pubmed/12636159.